Phase-controlling phononic crystal

N. Swinteck, J.F. Robillard, S. Bringuier, J. Bucay, K. Muralidharan, Jerome O. Vasseur, K. Runge, P.A. Deymier

Phase-controlling phononic crystal

Cite as: Appl. Phys. Lett. **98**, 103508 (2011); https://doi.org/10.1063/1.3559599
Submitted: 17 September 2010 • Accepted: 14 January 2011 • Published Online: 10 March 2011

N. Swinteck, J. -F. Robillard, S. Bringuier, et al.

Phase-controlling phononic crystal

N. Swinteck,[1,a)] J. -F. Robillard,[1] S. Bringuier,[1] J. Bucay,[1] K. Muralidharan,[1] J. O. Vasseur,[2] K. Runge,[1] and P. A. Deymier[1]
[1]*Department of Materials Science and Engineering, University of Arizona, Tucson, Arizona 85721, USA*
[2]*Institut d'Electronique, de Micro-électroniqueet de Nanotechnologie, UMR CNRS 8520, CitéScientifique, 59652 Villeneuve d'AscqCedex, France*

(Received 17 September 2010; accepted 14 January 2011; published online 10 March 2011)

We report on a phononic crystal (PC) consisting of a square array of cylindrical polyvinylchloride inclusions in air that can be used to control the relative phase of two incident acoustic waves with different incident angles. The phase shift between waves propagating through the crystal depends on the angle of incidence of the incoming waves and the PC length. The behavior of the PC is analyzed using the finite-difference-time-domain method. The band structure and equifrequency contours calculated via the plane wave expansion method show that the distinctive phase controlling properties are attributed to noncollinear wave and group velocity vectors in the PC as well as the degree of refraction. © *2011 American Institute of Physics*. [doi:10.1063/1.3559599]

Phononic crystals (PCs) are composite materials which derive their spectral (ω-space) and wave vector (k-space) properties from the scattering of elastic waves by periodic arrays of elastic inclusions embedded in an elastic matrix. Bulk or defected PCs have been shown to exhibit numerous useful spectral capabilities including transmission band gaps, local modes for guiding, filtering, and multiplexing.[1–15] k-space properties result from features in the band structure that impact refraction.[16–28] These properties parallel many of those found in photonic crystals.[29,30] The ω-space and k-space properties are directly related to the size, geometry, scale, and composition of the constitutive materials of the PC.

In the present letter, we demonstrate that the band structure of a two-dimensional PC constituted of a square array of cylindrical polyvinylchloride (PVC) inclusions in an air matrix can be used to control the relative phase of elastic waves. Phase control is due to the propagation of elastic waves in the PC with wave vectors that are not collinear with their group velocity vectors. This condition implies that excited Bloch waves travel at different phase velocities in the direction of their group velocity. Additionally, this crystal shows near zero-angle refraction permitting wave collimation as well as enabling the superposition of beams with different wave vectors in the same volume of crystal. Phase manipulation of these superposed waves can result in constructive or destructive interferences between noncollinear incident beams. Finally, there are operating frequencies for which the circular equifrequency contour (EFC) in air is larger than the first Brillouin zone of the PC, allowing several Bloch modes to exit the crystal, leading to the phenomenon of beam splitting. The work presented in this letter constitutes a significant move toward broadening the range of properties and applications of PCs beyond their more common spectral and wave number properties.

The PVC-air system parameters are: $\rho_{\mathrm{PVC}}=1364\ \mathrm{kg/m^3}$, $c_{t,\mathrm{PVC}}=1000\ \mathrm{m/s}$, $c_{l,\mathrm{PVC}}=2230\ \mathrm{m/s}$, $\rho_{\mathrm{AIR}}=1.3\ \mathrm{kg/m^3}$, $c_{t,\mathrm{AIR}}=0\ \mathrm{m/s}$, and $c_{l,\mathrm{AIR}}=340\ \mathrm{m/s}$, where ρ is density, c_t is transverse speed of sound, and c_l is longitudinal speed of sound. The inclusion radius is 12.9 mm and the lattice parameter is 27 mm. The plane wave expansion (PWE) method was employed to calculate the band structure of the PC (Ref. 6) [see Fig. 1(a)]. An extended zone scheme representation of a contour of the dispersion surface at 13.5 kHz is pictured in Fig. 1(b), consistent with the fourth band in Fig. 1(a), along with the EFCs of 13.5 kHz acoustic waves in air on the left and right hand sides. In this figure, an acoustic beam is directed at the PC face with incidence angle β_i. The k-vector component of the input that is parallel to the surface of the PC, k_y, is conserved at the interface and excites periodic Bloch modes in the k-space of the PC. The direction of energy propagation is along the gradient to the dispersion surface (group velocity vector) and is not parallel to the k-vector of the Bloch waves. The incident wave propagates

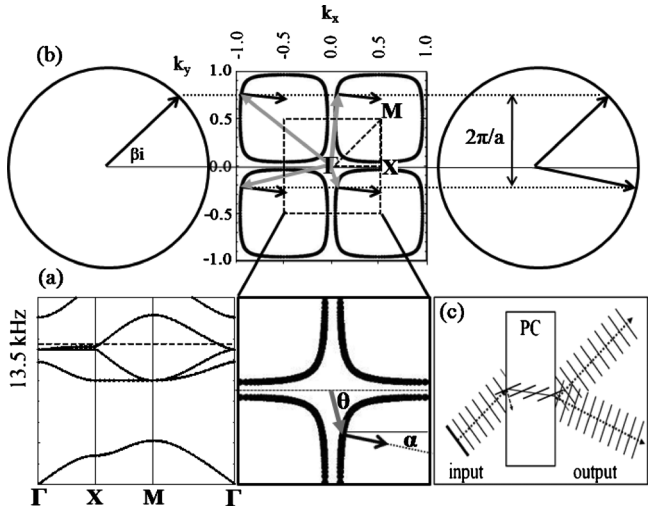

FIG. 1. (a) Band structure of PC generated by PWE method (Ref. 6) (b) Extended zone scheme and EFCs of air evaluated at 13.5 kHz (in units of $2\pi/a$). An incident acoustic signal with angle β_i impinging upon the crystal excites multiple Bloch modes via reciprocal lattice vector translation of a k-vector located within the first Brillouin zone. In the PC, the gray arrows represent wave vectors and the black arrows represent group velocity vectors. Bloch waves with parallel k-vector component coinciding with the EFC for air on the exit contribute to beam splitting. (c) Schematic representation of FDTD simulation domain.

a)Electronic mail: swinteck@email.arizona.edu.

from the left of the crystal to the right and only those waves inside the crystal that have a group velocity in that same direction will be excited. After propagation through the crystal, the k_y component of the wave vector is conserved at the interface between the PC and air and because the EFC in air is larger than the PC's first Brillouin zone, a split wave results. Positive refraction occurs at incident angles 2.3° to 28.1°, zero-angle refraction occurs at 28.1°, negative refraction occurs at angles from 28.1° to 74.5°. Angles below 2.3° or above 74.5° fall in the band gap and will be totally reflected. By symmetry of reciprocal space, negative input angles in the range 2.3°–28.1° and in the range 28.1°–74.5° will negatively refract and positively refract, respectively. For input angles in the ranges 15°–41° and −15°−−41°, the EFC has nearly flat faces and the beam will refract by less than 5°.

An analytical scheme and numerical scheme are used to quantify the phase shift developed in the PC for several *k*-vectors in reference to zero-angle refraction. The phase shift developed per length of crystal is dependent on the degree of refraction the incident wave experiences as well as the phase velocity associated with the wave vector in the PC. The distance a wave travels in the PC (the distance consistent with the path of the refracted beam) divided by the spacing between periodic peaks of high pressure coinciding with the orientation of its wave vector yields a value for the wave's phase. Comparing this value with a reference state yields Eq. (1)

$$\frac{\phi}{L} = |k_R|\cos(\theta_R) - \frac{|k_1|\cos(\theta_1 - \alpha_1)}{\cos(\alpha_1)}. \quad (1)$$

In Eq. (1), Φ is the phase shift developed within the PC between an arbitrary wave with *k*-vector k_1 and the reference wave corresponding to zero-angle refraction. L is the length of the crystal (distance between input side and output side) and α and θ are the angles made between the axis k_x and group velocity vector and wave vector, respectively [Figs. 1(b) and 1(c)]. We validate Eq. (1) using finite-difference-time-domain (FDTD) simulations. We send individual plane waves toward the PC and survey the displacement field at the entrance and at the exit to the PC over time. Relating the time evolution of the displacement field for these regions with the reference case of zero-angle refraction allows us to measure a phase shift for each incident angle. The discretization of space and time in the FDTD method leads to an uncertainty on calculated phase difference of approximately 0.027 radians. Agreement between Eq. (1) and FDTD results is seen in Fig. 2. Incidence angle and crystal length are the primary factors in controlling relative phase between propagating waves in the PC.

To demonstrate that the PC can effectively and precisely control phase, we simulate with FDTD two acoustic waves with incident angles of 10° and 28.1°. We desire to change the relative phase of these signals by π and 2π radians. The relative phase of the beams is characterized by taking cuts at the point of beam intersection before entry into the PC and at the point of beam intersection on the exit side of the crystal. We report the time average of the absolute value of instantaneous pressure over one period along these cuts (subsequently referred to as average pressure). If we observe a zero-value reading at the mid-point along the cut, destructive interference has occurred between the beams corresponding

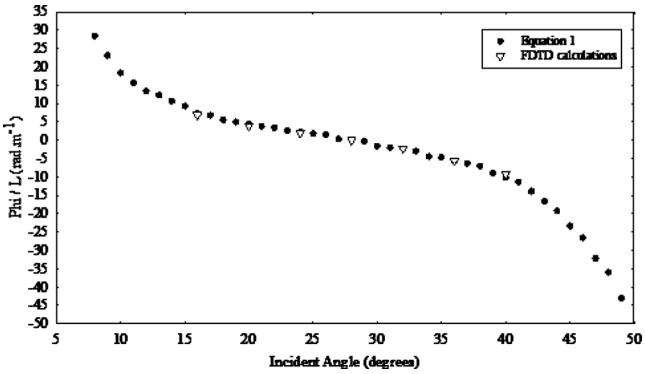

FIG. 2. Phase shift per PC length in reference to the zero-angle refraction angle of 28.1°. The solid black dots represent analytical results from Eq. (1) and the unfilled triangles represent FDTD calculations. The FDTD results are obtained with a crystal of length 540 mm (20 lattice parameters). The uncertainty on calculated phase difference in FDTD calculations is 0.027 radians.

to a π phase shift. If we observe a maximum-value reading, the phase shift is 2π and constructive interference has occurred. From the exit side of the crystal to the point of beam intersection, there is an additional phase shift developed between the beams because they travel different paths to reach the point where the average pressure cut is taken. This component must be included into calculations such that a true phase change of π and 2π can be realized of the system. For a PC of length 23 lattice parameters (621 mm), the PC initiates a relative phase shift of 11.404 radians between the waves. The additional, outside phase contribution is 14.515 radians. The difference in these values gives the total phase change between the two acoustic inputs for the system, this value is approximately π. For a PC of length 46 lattice parameters (1242 mm), the PC initiates a relative phase shift of 22.808 radians between the waves. The outside phase contribution is 29.031 radians and the difference (total phase change) is roughly 2π radians. Figure 3(a) shows the 10° and 28.1° sources interacting with the shorter crystal. In that figure, we show 2 black lines indicating where cuts are taken. In Fig. 3(b), we report the profiles of the average pressure along these cuts. On the entry side of the PC, a zero pressure reading at the point of beam intersection [Fig. 3(b)] shows that the sources are initially out-of-phase. The average pressure along the cut on the backside of the crystal shows a maximum at its mid-point. The exit beams are in-phase and a total phase shift of π has been measured. Figures 3(c) and 3(d) show the 10° and 28.1° sources interacting with the longer PC. As before, the incident beams are π out-of-phase. On the exit side of the PC, instead of getting a maximum-value reading as was the case with the shorter crystal, we observe a zero-value reading of the average pressure at the mid-point. A total phase shift of 2π has been measured. These results demonstrate that based solely on the selection of incident angle and crystal length, phase can be manipulated.

We illustrate the possibility of phase control by another example (Fig. 4). We note that incident angles of –32° and 24° excite the same Bloch waves in the PC. The signals travel the same path through the PC as one, superposed, collimated beam and exit at the same location on the backside of the crystal. An initial relative phase difference between the two waves of π, as in Fig. 4(a), results in destruc-

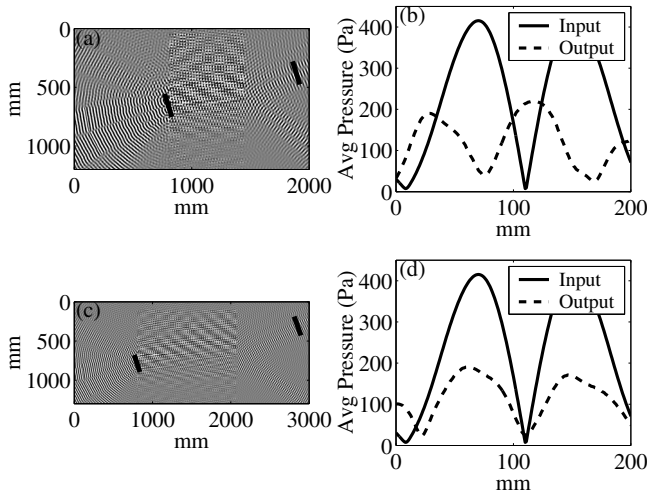

FIG. 3. (a) FDTD instantaneous pressure plot of the simulation domain with two incident beams at 10° and 28.1° impinging on a PC with dimensions 1350 mm × 621 mm (50 × 23 lattice parameters). The time average of the absolute value of instantaneous pressure over one period (referred to as average pressure) is calculated along two spatial cuts indicated as solid black lines. (b) Profile of average pressure taken along cuts in (a). (c) FDTD instantaneous pressure plot of simulation domain with two incident beams at 10° and 28.1° impinging on PC with dimensions 1350 mm × 1242 mm (50 × 46 lattice parameters). (d) Profile of average pressure taken along cuts in (c).

tive interference. The beams cancel and a very weak pressure field is seen on the exit side of the PC. This nonzero pressure field is due to mismatch loss. Conversely, with no phase difference between the input beams, the waves interfere constructively along all paths of travel and produce two intense beams upon exit [Fig. 4(b)]. This situation is unique in the manner that the crystal length has no effect on the relative phase of the two signals.

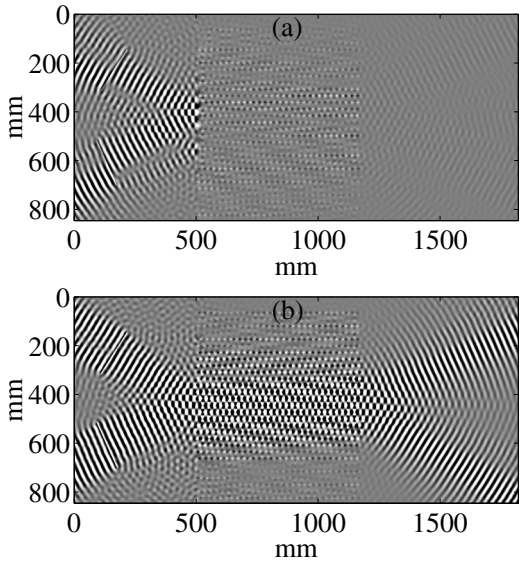

FIG. 4. FDTD instantaneous pressure plot of simulation domain with two incident beams at −32° and 24° impinging on PC with dimensions 810 mm × 621 mm (30 × 23 lattice parameters). The input waves excite the same Bloch waves within the PC. For a π radian phase shift between the incident beams there is destructive interference along all paths of travel (a) and for zero phase shift there is constructive interference along all paths of travel (b).

We have evaluated a PC that possesses passing bands exhibiting unusual k-space properties that depend on the angle of incidence of an incoming wave leading to the possibility of controlling the phase of waves propagating through the crystal. This PC offers control over the full phase space of waves, namely, ω-space, k-space, and Φ-space.

We gratefully acknowledge support from NSF under Grant No. 0924103.

[1]J. O. Vasseur, B. Djafari-Rouhani, L. Dobrzynski, M. S. Kushwaha, and P. Halevi, J. Phys.: Condens. Matter **6**, 8759 (1994).
[2]M. M. Sigalas and E. N. Economou, Solid State Commun. **86**, 141 (1993).
[3]J. O. Vasseur, B. Djafari-Rouhani, L. Dobrzynski, and P. A. Deymier, J. Phys.: Condens. Matter **9**, 7327 (1997).
[4]E. N. Economou and M. M. Sigalas, Phys. Rev. B **48**, 13434 (1993); J. Acoust. Soc. Am. **95**, 1734 (1994).
[5]M. S. Kushwaha, P. Halevi, L. Dobrzynski, and B. Djafari-Rouhani, Phys. Rev. Lett. **71**, 2022 (1993).
[6]M. S. Kushwaha, B. Djafari-Rouhani, L. Dobrzynski, and J. O. Vasseur, Eur. Phys. J. B **3**, 155 (1998).
[7]M. Kafesaki and E. N. Economou, Phys. Rev. B **60**, 11993 (1999).
[8]I. E. Psarobas, N. Stefanou, and A. Modinos, Phys. Rev. B **62**, 278 (2000).
[9]Z. Liu, C. T. Chan, P. Sheng, A. L. Goertzen, and J. H. Page, Phys. Rev. B **62**, 2446 (2000).
[10]Z. Liu, X. Zhang, Y. Mao, Y. Y. Zhu, Z. Yang, C. T. Chan, and P. Sheng, Science **289**, 1734 (2000).
[11]M. Torres, F. R. Montero de Espinosa, and J. L. Aragon, Phys. Rev. Lett. **86**, 4282 (2001).
[12]J. O. Vasseur, P. A. Deymier, B. Chenni, B. Djafari-Rouhani, L. Dobrzynski, and D. Prevost, Phys. Rev. Lett. **86**, 3012 (2001).
[13]J. H. Page, A. L. Goertzen, S. Yang, Z. Liu, C. T. Chan, and P. Sheng, in *Photonic Crystals and Light Localization in the 21st Century*, NATO Advanced Studies Institute, Series C: Mathematical and Physical Sciences Vol. 563, edited by C. M. Soukoulis (Kluwer, Dordrecht, 2002), p. 59.
[14]S. Yang, J. H. Page, Z. Liu, M. L. Cowan, C. T. Chan, and P. Sheng, Phys. Rev. Lett. **88**, 104301 (2002).
[15]J. H. Page, S. Yang, M. L. Cowan, Z. Liu, C. T. Chan, and P. Sheng, *Wave Scattering in Complex Media: From Theory to Applications*, NATO Science Series, edited by B. A. van Tiggelen and S. Skipetrov (Kluwer Academic, Amsterdam, 2003), p. 283.
[16]S. Yang, J. H. Page, Z. Liu, M. L. Cowan, C. T. Chan, and P. Sheng, Phys. Rev. Lett. **93**, 024301 (2004).
[17]J. H. Page, A. Sukhovich, S. Yang, M. L. Cowan, F. Van der Biest, A. Tourin, M. Fink, Z. Liu, C. T. Chan, and P. Sheng, Phys. Status Solidi B **241**, 3454 (2004).
[18]K. Imamura and S. Tamura, Phys. Rev. B **70**, 174308 (2004).
[19]X. Zhang and Z. Liu, Appl. Phys. Lett. **85**, 341 (2004).
[20]J. Li, K. H. Fung, Z. Y. Liu, P. Sheng, and C. T. Chan, *Physics of Negative Refraction and Negative Index Materials*, Springer Series in Materials Science Vol. 98 (Springer Berlin, Heidelberg, 2007), Chap. 8.
[21]M. Ke, Z. Liu, Z. Cheng, J. Li, P. Peng, and J. Shi, Solid State Commun. **142**, 177 (2007).
[22]A. Sukhovich, L. Jing, and J. Page, Phys. Rev. B **77**, 014301 (2008).
[23]A. Sukhovich B. Merheb, K. Muralidharan, J. O. Vasseur, Y. Pennec, P. A. Deymier, and J. H. Page, Phys. Rev. Lett. **102**, 154301 (2009).
[24]J. S. Shi, S. S. Lin, and T. J. Huang, Appl. Phys. Lett. **92**, 111901 (2008).
[25]J. Bucay, E. Roussel, J. O. Vasseur, P. A. Deymier, A.-C. Hladky-Hennion, Y. Pennec, K. Muralidharan, B. Djafari-Rouhani, and B. Dubus, Phys. Rev. B **79**, 214305 (2009).
[26]J. Witzens, M. Loncar, and A. Scherer, IEEE J. Sel. Top. Quantum Electron. **8**, 1246 (2002).
[27]D. N. Chigrin, S. Enoch, C. M. S. Torres, and G. Tayeb, Opt. Express **11**, 1203 (2003).
[28]P. T. Rakich, M. S. Dahlem, S. Tandon, M. Ibanescu, M. Soljacic, G. S. Petrich, J. D. Joannopoulos, L. A. Kolodziejski, and E. P. Ippen, Nature Mater. **5**, 93 (2006).
[29]H. Kosaka, T. Kawashima, A. Tomita, M. Notomi, T. Tamamura, T. Sato, and S. Kawakami, Appl. Phys. Lett. **74**, 1370 (1999).
[30]J. Shi, B. K. Juluri, S.-C. S. Lin, M. Lu, T. Gao, and T. J. Huang, J. Appl. Phys. **108**, 043514 (2010).